ChemComm

COMMUNICATION

View Article Online
View Journal | View Issue

Cite this: *Chem. Commun.*, 2019, **55**, 10230

Received 15th July 2019,
Accepted 30th July 2019

DOI: 10.1039/c9cc05436g

rsc.li/chemcomm

Structure and thermal expansion of the distorted Prussian blue analogue $RbCuCo(CN)_6$†

Hanna L. B. Boström *[ab] and Ronald I. Smith [c]

The structure and thermal expansion of the Prussian blue analogue $RbCuCo(CN)_6$ has been determined *via* neutron and X-ray powder diffraction. The system crystallises in *Cccm* and harbours three coexisting distortions relative to the parent $Fm\bar{3}m$ structure, which leads to anisotropic thermal expansion with a near-zero component in one direction. The difficulties associated with determining octahedral tilt systems in Prussian blue analogues and related double molecular perovskites are discussed.

Prussian blue analogues (PBAs) are a class of cyanide-linked coordination polymers with general formula $A_xM[M'(CN)_6]_y$ and high-symmetry parent space group $Fm\bar{3}m$. The composition is variable and ranges from stoichiometric, A-site deficient $M[M'(CN)_6]$ to defective $M[M'(CN)_6]_y$ ($y < 1$) or cation-containing $AM[M'(CN)_6]$, depending on the charges on the metals.[1–3] The two transition metals M and M′ are both octahedrally coordinated and form a 3D framework analogous to double perovskites ($A_2BB'X_6$). This article focuses on the composition $AMM'(CN)_6$, where only half of the cubic interstices ("A-sites" in perovskite terminology) are occupied by cations. PBAs can be considered a subset of so-called molecular or hybrid perovskites,[4,5] which are characterised by high flexibility and additional degrees of freedom in comparison to conventional oxide perovskites.[6–8] For example, the octahedra can rotate in phase in directions perpendicular to the rotation axis or translate cooperatively in columns or layers, denoted "unconventional" tilting and columnar shifts, respectively.[6,7,9] Many molecular perovskites—*e.g.* azides,[10] hypophosphites,[11] or formates[12]—are very flexible and predominantly adopt distorted low-symmetry (hettotype) structures. Although cubic space groups dominate for PBAs,[13,14] symmetry-lowering distortions occur under certain conditions and can act as useful design elements for crystal engineering. For example, the inclusion of Jahn–Teller active cations in $CuPt(CN)_6$ lowers the symmetry to tetragonal $I4/mmm$, which significantly alters the thermal expansion and compressibility.[15,16] Moreover, octahedral tilting—as is well known in perovskites—can be induced by external or chemical pressure and has been shown to both improve the ionic transport properties and enhance the magnetic ordering temperature.[16–19]

However, unlike many molecular perovskites, relatively few PBAs exhibit more than one structural distortion. Coexistence of distortions is important, as it provides a potential avenue for the development of polar structures by improper ferroelectricity, as reported for other molecular perovskites.[20–22] Yet, some multiply distorted PBAs are known and they often show interesting features. To illustrate, the charge-transfer system $RbMnFe(CN)_6$ contains both alternating occupational Rb order and Jahn–Teller distortions, which reduces the symmetry to the piezoelectric space group $I\bar{4}m2$.[23] Ferromagnetism and ferroelectricity have been demonstrated for a similar composition.[24] A related, distorted PBA is $RbCuFe(CN)_6$, where the departure from $Fm\bar{3}m$ symmetry is described by three distortions: octahedral tilting, Rb order, and Jahn–Teller distortions.[25] Structure determination is typically performed using powder X-ray diffraction (PXRD), but this does not accurately probe Jahn–Teller distortions and tilts, as these modes only manifest in the positions of the weakly scattering cyanide ions. This motivates the present study, where we use X-ray and neutron powder diffraction to study the previously unreported $RbCuCo(CN)_6$, which is presumably isostructural to the hexacyanoferrate mentioned above. This manuscript discusses the structural distortions and their effect on the thermal expansion followed by a discussion about the difficulties encountered when determining tilt systems for PBAs.

It is convenient to describe the symmetry-lowering distortion by means of an irreducible representation (irrep) with respect to parent space group. Irreps in cubic periodic structures assume the

[a] *Department of Chemistry, Ångström Laboratory, Uppsala University, Box 538, 751 21 Uppsala, Sweden. E-mail: hanna.bostrom@kemi.uu.se*
[b] *Department of Chemistry, Inorganic Chemistry Laboratory, University of Oxford, South Parks Road, Oxford OX1 3QR, UK*
[c] *ISIS Facility, Rutherford Appleton Laboratory, Harwell Campus, Didcot OX11 0QX, UK*

† Electronic supplementary information (ESI) available: Experimental details, crystallographic details, and supplementary group-theoretical discussions. See DOI: 10.1039/c9cc05436g

form $k_{\#}^{\pm}$, where k denotes the periodicity of the distortion. The exact form of the irrep is dependent on the origin choice and here, the origin is located at one of the transition metals (B-site in perovskite terminology) throughout. For a conversion to other settings, see ref. 22.

$RbCuCo(CN)_6$ was prepared by carefully placing 2 ml of an aqueous solution of $CuCl_2$ (67.2 mg, 0.5 mmol) on top of 2 ml of an aqueous solution of $K_3Co(CN)_6$ (166.2 mg, 0.5 mmol) saturated with RbCl. The reaction was left undisturbed for 1 day, followed by vigorous mixing and the pale blue solid collected by filtration *in vacuo*. Yields were in the range 69–79% based on $CuCl_2$. The sample composition was verified by energy-dispersive X-ray spectroscopy (EDX) to be $Rb_{0.90}Cu[Co(CN)_6]_{0.92}$. The water content was estimated from thermogravimetric analysis as 3–5 water molecules per formula unit. 5 batches were combined for the neutron diffraction measurement and data analysis was carried out by symmetry-mode Rietveld refinement as implemented in the softwares TOPAS and ISODISTORT.[26–28] Further details about the characterisation are given in the ESI.†

Indexing of the PXRD pattern collected at ambient conditions suggested the space group *Ccc*2 with cell parameters $a \sim 10.9$ Å, $b \sim 9.99$ Å and $c \sim 10.03$ Å (note that a and b are interchangeable in this space group). As PBAs are rarely polar, the centrosymmetric minimal subgroup *Cccm*—which has an identical diffraction pattern—was used for refinement. This differs from the *Pmna* symmetry reported for $RbCuFe(CN)_6$,[25] which is a maximal subgroup of *Cccm*. Therefore, the structure reported for $RbCuFe(CN)_6$ is possibly solved in a space group with too low symmetry. Group-theoretical analysis using ISODISTORT[27] indicates that the symmetry lowering from $Fm\bar{3}m$ to *Cccm* arises from a superposition of three modes: a Jahn–Teller distortion (irrep Γ_3^+), an octahedral tilt (irrep X_3^+) and a rod-like occupational order of the Rb cations (irrep X_4^+). The combination of any two of these distortions gives the third as a secondary order parameter, hence it is sufficient to specify two of these distortion modes. In other words, the cation order can be said to arise from the combination of the Jahn–Teller distortion and the tilt, or *vice versa* that the tilt results from the Jahn–Teller distortion and the cation order. The extent to which the third mode is activated will depend on the energies of the three modes, but such information is not available using group-theoretical methods. This coupling can also be inferred by comparing $RbCuCo(CN)_6$ to the $P\bar{4}n2$ phase of $RbMnFe(CN)_6$.[23] The latter has no Jahn–Teller distortion and therefore also lacks the Rb order, despite possessing the X_3^+ tilt present in $RbCuCo(CN)_6$.

Symmetry-mode refinement against neutron diffraction data [Fig. 1] gives accurate information about the relative magnitude of the three distortions. The most striking distortion is the occupational order of the A-site Rb cations, which also induces a small deformation of the octahedra. This type of order also appears in $RbCuFe(CN)_6$, but is otherwise less prevalent than the alternating pattern (irrep R_2^-), giving $F\bar{4}3m$ symmetry.[23,29,30] The strongest displacive mode—as calculated by the software AMPLIMODES[31]—is the octahedral tilt described by $a^0a^0c^+$ in Glazer notation,[32] *i.e.* an in-phase tilt

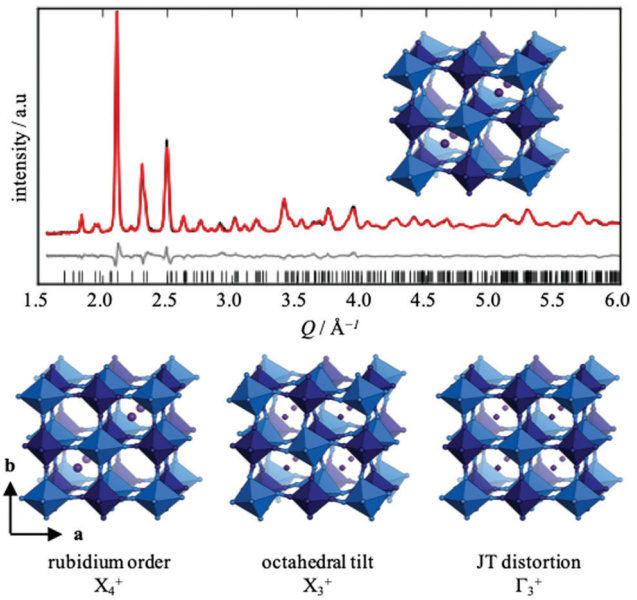

Fig. 1 Powder neutron diffraction pattern for $RbCuCo(CN)_6$ from detector bank 4 at the GEM diffractometer, ISIS. The Rietveld fit is shown in red, the difference curve (data−fit) in grey and allowed reflections are indicated by vertical bars. The three constituent distortions and their irreps are also shown.

polarised along a single axis. This tilt system is relatively infrequent in PBAs, where the dominant tilt patterns are $a^-a^-a^-$ or $a^-a^-c^+$,[16,33–36] yet has a precedent in the metastable $P\bar{4}n2$ phase of $RbMnFe(CN)_6$.[23] It is a conventional tilt pattern, unlike the unconventional tilt—where neighbouring octahedra rotate perpendicular to the rotation axis tilt in the same sense[7,9]—present in the original *Pmna* structure for $RbCuFe(CN)_6$ suggested by Matsuda and coworkers.[25] Finally, the cooperative Jahn–Teller effect manifests as a cooperative elongation of the CuN_6 octahedra along a, and mirrors that of $CuPt(CN)_6$, $ACuFe(CN)_6$ (A = Cs or Rb) and the low-temperature form of $RbMnFe(CN)_6$.[15,25,37] In Jahn–Teller active formates and perovskite oxides, several distinct periodicities of the cooperative Jahn–Teller order are possible,[38,39] whereas defect-free Jahn–Teller-active PBAs always show in-phase arrangements ($\mathbf{k} = [0, 0, 0]$) of the long axes.[15,40] This gives a macroscopic symmetry lowering, in contrast to most defective Cu-containing systems, which tend to adopt the cubic aristotype symmetry.[41,42] Since A-site cations and vacancies compete, the inclusion of Rb in the title compound prevents the formation of vacancies and so leads to Jahn–Teller order. As these examples highlight, all of the distortions present in $RbCuCo(CN)_6$ are precedented, yet they rarely coexist.

The thermal dependence of the lattice parameters was monitored in the range 100–500 K using high-resolution PXRD and the thermal expansion coefficients calculated by PASCal [Fig. 2].[43] $RbCuCo(CN)_6$ shows an anisotropic thermal response, which can be interpreted in terms of the structural distortions. The expansivity is positive in the *ab*-plane, with the largest magnitude in the **a** direction of 31.5(6) M K^{-1} and a smaller value of 4.29(13) M K^{-1} along **b**. These values are within the range observed for the magnitude of the thermal expansion coefficients in other PBAs.[44] The thermal expansion along the

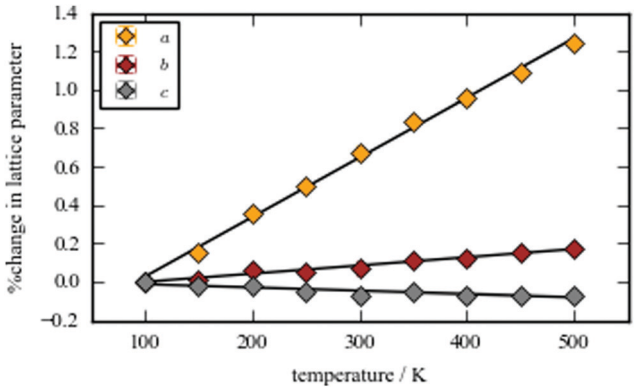

Fig. 2 The percentage change of the lattice parameters as a function of temperature, along with lines of best fit.

c direction—where the Cu–N–C–Co linkages are linear on average—is negative and very small ($-1.7(3)$ M K^{-1}). This suggests the presence of a low-energy transverse phonon; a known cause of negative thermal expansion (NTE) in framework materials.[45] As a result, further phase transitions may be expected on cooling, as the soft mode condenses. Although NTE is a relatively rare phenomenon in general, it frequently appears in Prussian blue analogues, although there is a strong dependence on the metal composition.[15,44] The thermal expansion is consistent with a decrease in the tilting angles upon heating and suggests that the tilting vanishes at even higher temperatures.

The determination of tilts in double molecular perovskites from the space group symmetry can be challenging. In simple (ABX_3) perovskites, distortions with periodicity $\mathbf{k} = \left\langle 0, 0, \frac{1}{2} \right\rangle$ and $\mathbf{k} = \left\langle 0, \frac{1}{2}, \frac{1}{2} \right\rangle$ transform as different irreps, labelled X and M, respectively. However, in face-centred double perovskites ($A_2BB'X_6$), these points in reciprocal space are equivalent by symmetry and so result in the same space group (see ESI† for further discussion). Thus, determination of the correct space group does not uniquely define the tilt pattern [Fig. 3]. By way of example, the space group *P*4/*mbm* is usually a signature of in-phase tilting ($a^0a^0c^+$) for a simple perovskite.[46] In a double perovskite, this tilt system instead drives *P*4/*mnc* symmetry,[47] yet in molecular double perovskites—which have more degrees of freedom—this space group can also arise from the unconventional tilt system described by

$$\begin{bmatrix} 0 & 0 & 0 \\ 0 & 0 & 0 \\ + & + & - \end{bmatrix}, \qquad (1)$$

according to the notation developed in ref. 9. The "+" signs denote in-phase tilting in directions perpendicular to the rotation axis and is unfeasible in conventional oxide perovskites. As a result, tilt systems cannot be assigned for double molecular perovskites based on space group alone, as is often possible for simple oxide perovskites. Care must be exerted

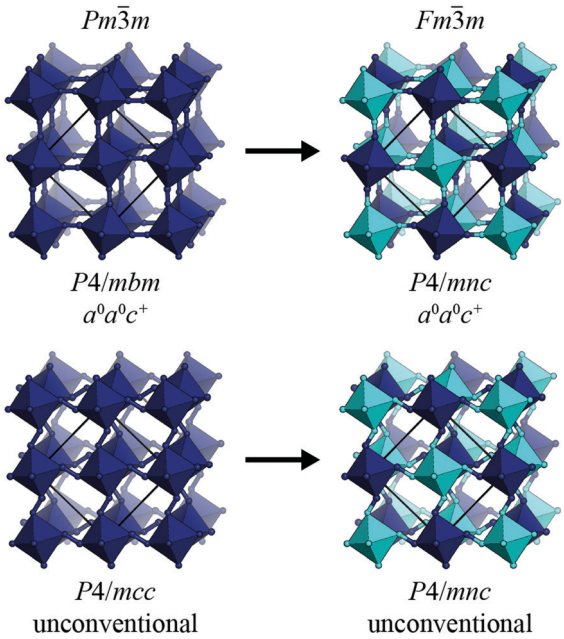

Fig. 3 The tilt modes on the left hand side drive different space group symmetries when acting on a simple perovskite-like framework (BX_3). Conversely, in the case of double perovskites ($BB'X_6$), the tilt distortions yield the same space group, *P*4/*mnc*. Unit cells are indicated by black lines and A-site cations are omitted.

during structure determination from PXRD data, as the two different tilt systems will give very similar qualities of fits to the data, given the weak scattering power of the cyanide anions. This analysis (unsurprisingly) highlights the need for more neutron diffraction studies on distorted Prussian blue analogues as well as other double molecular perovskites, such as thiocyanates and formates.[48–50]

To summarise, the structure of the Prussian blue analogue $RbCuCo(CN)_6$ has been studied with X-ray and neutron powder diffraction. The system exhibits rod-like occupational rubidium order, octahedral tilts and Jahn–Teller distortions, which together reduce the symmetry from the parent space group *Fm*3̄*m* to *Cccm*. Although distorted Prussian blue analogues are known, coexistence of several distortions is less common, but is a prerequisite for *e.g.* the development of hybrid improper ferroelectricity.[20,22] Group-theoretical analysis highlights the coupling of the three distortions, where the presence of two induces the third. The potential problems associated with the determination of tilt systems for Prussian blue analogues highlighted here have implications for research on both PBAs and other systems in a large number of fields. In particular, tilting is often encountered for A-site containing PBAs, which are of currency for their performance as positive electrode materials in Na ion batteries.[51,52]

We thank the ISIS neutron and muon source for Xpress beamtime at the GEM diffractometer (data DOI: 10.5286/ISIS.E.RB1990103).[53] High-resolution XRD was carried out at I11, Diamond Light Source, UK under the allocation of a Block Award Group award EE18786. Assistance from W. R. Brant (Uppsala) with synthesis, D. Karlsson (Uppsala) with EDX measurements,

A. Gibbs (ISIS) with data collection, and S. J. Cassidy (Oxford) with data analysis is greatly appreciated. M. S. Senn (Warwick) is acknowledged for useful discussions.

Conflicts of interest

There are no conflicts to declare.

Notes and references

1 H.-J. Buser, G. Ron and A. Ludi, *J. Chem. Soc., Faraday Trans.*, 1974, 2473–2474.
2 H. J. Buser, D. Schwarzenbach, W. Petter and A. Ludi, *Inorg. Chem.*, 1977, **16**, 2704–2710.
3 A. Bleuzen, C. Lomenech, V. Escax, F. Villain, F. Varret, C. Cartier dit Moulin and M. Verdaguer, *J. Am. Chem. Soc.*, 2000, **122**, 6648–6652.
4 G. Kieslich and A. L. Goodwin, *Mater. Horiz.*, 2017, **4**, 362–366.
5 W. Li, Z. Wang, F. Deschler, S. Gao, R. H. Friend and A. K. Cheetham, *Nat. Rev. Mater.*, 2017, **2**, 16099.
6 H. L. B. Boström, J. A. Hill and A. L. Goodwin, *Phys. Chem. Chem. Phys.*, 2016, **18**, 31881–31894.
7 S. G. Duyker, J. A. Hill, C. J. Howard and A. L. Goodwin, *J. Am. Chem. Soc.*, 2016, **138**, 11121–11123.
8 W. Zhang, Y. Cai, R.-G. Xiong, H. Yoshikawa and K. Awaga, *Angew. Chem., Int. Ed.*, 2010, **49**, 6608–6610.
9 J. A. Hill, A. L. Thompson and A. L. Goodwin, *J. Am. Chem. Soc.*, 2016, **138**, 5886–5896.
10 X.-H. Zhao, X.-C. Huang, S.-L. Zhang, D. Shao, H.-Y. Wei and X.-Y. Wang, *J. Am. Chem. Soc.*, 2013, **135**, 16006–16009.
11 Y. Wu, T. Binford, J. A. Hill, S. Shaker, J. Wang and A. K. Cheetham, *Chem. Commun.*, 2018, **54**, 3751–3754.
12 X.-Y. Wang, L. Gan, S.-W. Zhang and S. Gao, *Inorg. Chem.*, 2004, **43**, 4615–4625.
13 J. Balmaseda, E. Reguera, J. Rodríguez-Hernández, L. Reguera and M. Autie, *Microporous Mesoporous Mater.*, 2006, **96**, 222–236.
14 J. Roque, E. Reguera, J. Balmaseda, J. Rodríguez-Hernández, L. Reguera and L. F. del Castillo, *Microporous Mesoporous Mater.*, 2007, **103**, 57–71.
15 K. W. Chapman, P. J. Chupas and C. J. Kepert, *J. Am. Chem. Soc.*, 2006, **128**, 7009–7014.
16 H. L. B. Boström, I. E. Collings, A. B. Cairns, C. P. Romao and A. L. Goodwin, *Dalton Trans.*, 2019, **48**, 1647–1655.
17 X. Liu, Y. Moritomo, T. Matsuda, H. Kamioka, H. Tokoro and S.-I. Ohkoshi, *J. Phys. Soc. Jpn.*, 2009, **78**, 013602.
18 M. Sugimoto, S. Yamashita, H. Akutsu, Y. Nakazawa, J. G. DaSilva, C. M. Kareis and J. S. Miller, *Inorg. Chem.*, 2017, **56**, 10452–10457.
19 Y. Xu, J. Wan, L. Huang, M. Ou, C. Fan, P. Wei, J. Peng, Y. Liu, Y. Qiu, X. Sun, C. Fang, Q. Li, J. Han, Y. Huang, J. A. Alonso and Y. Zhao, *Adv. Energy Mater.*, 2019, **9**, 1803158.
20 N. A. Benedek and C. J. Fennie, *Phys. Rev. Lett.*, 2011, **106**, 107204.
21 A. Stroppa, P. Jain, P. Barone, M. Marsman, J. M. Perez-Mato, A. K. Cheetham, H. W. Kroto and S. Picozzi, *Angew. Chem., Int. Ed.*, 2011, **50**, 5847–5850.
22 H. L. B. Boström, M. S. Senn and A. L. Goodwin, *Nat. Commun.*, 2018, **9**, 2380.
23 Y. Moritomo, M. Hanawa, Y. Ohishi, K. Kato, M. Takata, A. Kuriki, E. Nishibori, M. Sakata, S. Ohkoshi, H. Tokoro and K. Hashimoto, *Phys. Rev. B: Condens. Matter Mater. Phys.*, 2003, **68**, 144106.
24 S.-i. Ohkoshi, H. Tokoro, T. Matsuda, H. Takahashi, H. Irie and K. Hashimoto, *Angew. Chem., Int. Ed.*, 2007, **46**, 3238–3241.
25 T. Matsuda, J. Kim and Y. Moritomo, *Dalton Trans.*, 2012, **41**, 7620–7623.
26 H. M. Rietveld, *Acta Crystallogr.*, 1967, **22**, 151–152.
27 B. J. Campbell, H. T. Stokes, D. E. Tanner and D. M. Hatch, *J. Appl. Crystallogr.*, 2006, **39**, 607–614.
28 A. A. Coelho, *TOPAS-Academic, version 4.1 (computer software), Coelho Software*, Brisbane, 2007.
29 E. J. M. Vertelman, T. T. A. Lummen, A. Meetsma, M. W. Bouwkamp, G. Molnar, P. H. M. van Loosdrecht and P. J. van Konigsbruggen, *Chem. Mater.*, 2008, **20**, 1236–1238.
30 T. Nuida, T. Matsuda, H. Tokoro, S. Sakurai, K. Hashimoto and S.-I. Ohkoshi, *J. Am. Chem. Soc.*, 2005, **127**, 11604–11605.
31 D. Orobengoa, C. Capillas, M. I. Aroyo and J. M. Perez-Mato, *J. Appl. Crystallogr.*, 2009, **42**, 820–833.
32 A. M. Glazer, *Acta Crystallogr., Sect. B: Struct. Crystallogr. Cryst. Chem.*, 1972, **28**, 3384–3392.
33 C. M. Kareis, S. H. Lapidus, J.-H. Her, P. W. Stephens and J. S. Miller, *J. Am. Chem. Soc.*, 2012, **134**, 2246–2254.
34 J.-H. Her, P. W. Stephens, C. M. Kareis, J. G. Moore, K. S. Min, J.-W. Park, G. Ball, B. S. Kennon and J. S. Miller, *Inorg. Chem.*, 2010, **49**, 1524–1534.
35 J. Song, L. Wang, Y. Lu, J. Liu, B. Guo, P. Xiao, J.-J. Lee, X.-G. Yang, G. Henkelman and J. B. Goodenough, *J. Am. Chem. Soc.*, 2015, **137**, 2658–2664.
36 X. Bie, K. Kubota, T. Hosaka, K. Chihara and S. Komaba, *J. Mater. Chem. A*, 2017, **5**, 4325–4330.
37 H. Tokoro, S.-i. Ohkoshi, T. Matsuda and K. Hashimoto, *Inorg. Chem.*, 2004, **43**, 5231–5236.
38 K.-L. Hu, M. Kurmoo, Z. Wang and S. Gao, *Chem. – Eur. J.*, 2009, **15**, 12050–12064.
39 E. Sletten and L. H. Jensen, *Acta Crystallogr., Sect. B: Struct. Crystallogr. Cryst. Chem.*, 1973, **29**, 1752–1756.
40 W. Kosaka, T. Ishihara, H. Yashiro, Y. Taniguchi, K. Hashimoto and S.-I. Ohkoshi, *Chem. Lett.*, 2005, **34**, 1278–1279.
41 E. Reguera, J. Rodríguez-Hernández, A. Champi, J. G. Duque, E. Granado and C. Rettori, *Z. Phys. Chem.*, 2006, **220**, 1609–1619.
42 J. Jiménez-Gallegos, J. Rodríguez-Hernández, H. Yee-Madeira and E. Reguera, *J. Phys. Chem. C*, 2010, **114**, 5043–5048.
43 M. J. Cliffe and A. L. Goodwin, *J. Appl. Crystallogr.*, 2012, **45**, 1321–1329.
44 S. Adak, L. L. Daemen, M. Hartl, D. Williams, J. Summerhill and H. Nakotte, *J. Solid State Chem.*, 2011, **184**, 2854–2861.
45 J. S. O. Evans, *J. Chem. Soc., Dalton Trans.*, 1999, 3317–3326.
46 C. J. Howard and H. T. Stokes, *Acta Crystallogr., Sect. B: Struct. Sci.*, 1998, **54**, 782–789.
47 C. J. Howard, B. J. Kennedy and P. M. Woodward, *Acta Crystallogr., Sect. B: Struct. Sci.*, 2003, **59**, 463–471.
48 M. J. Cliffe, E. N. Keyzer, M. T. Dunstan, S. Ahmad, M. F. L. De Volder, F. Deschler, A. J. Morris and C. P. Grey, *Chem. Sci.*, 2019, **10**, 793–801.
49 K.-P. Xie, W.-J. Xu, C.-T. He, B. Huang, Z.-Y. Du, Y.-J. Su, W.-X. Zhang and X.-M. Chen, *CrystEngComm*, 2016, **18**, 4495–4498.
50 M. Mączka, B. Bondzior, P. Dereń, A. Sieradzki, J. Trzmiel, A. Pietraszko and J. Hanuza, *Dalton Trans.*, 2015, **44**, 6871–6879.
51 L. Wang, J. Song, R. Qiao, L. A. Wray, M. A. Hossain, Y.-D. Chuang, W. Yang, Y. Lu, D. Evans, J.-J. Lee, S. Vail, X. Zhao, M. Nishijima, S. Kakimoto and J. B. Goodenough, *J. Am. Chem. Soc.*, 2015, **137**, 2548–2554.
52 C. Fang, Y. Huang, W. Zhang, J. Han, Z. Deng, Y. Cao and H. Yang, *Adv. Energy Mater.*, 2016, **6**, 1501727.
53 W. G. Williams, R. M. Ibberson, P. Day and J. E. Enderby, *Phys. B*, 1998, **241–243**, 234–236.